

**Supplemental Figure 1.** A. Protocol for testing PARPi-FL staining, and PARP1-immunofluorescence with H&E in thin sections, B. Protocol for staining whole specimens with PARPi-FL followed by RCM-FCM imaging, C. Protocol for permeability studies in mastectomy specimens in human ex vivo tissue, D. Protocol for PARPi-FL staining in live anesthetized pigs

**Supplemental Figure 2.** A. Representative example of a thin section annotated by a pathologist, B-D. Representative example of PARP1 IHC along with corresponding H&E in superficial, nodular and infiltrative BCCs, three examples are presented from each subtype. High PARP1 expression is seen in all BCCs, irrespective of subtype, E. Example of heterogenous PARP1 expression

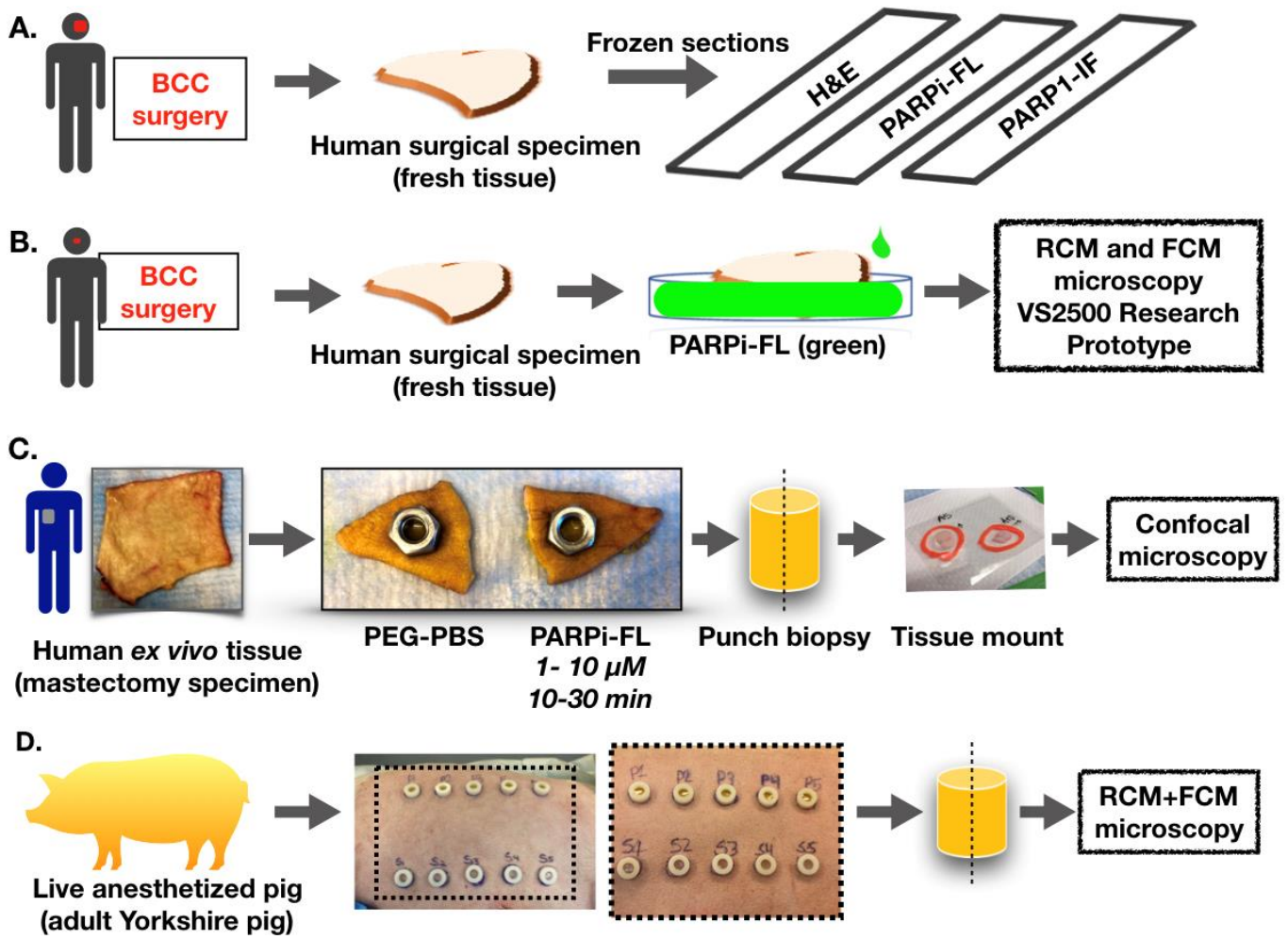
**Supplemental Figure 3.** A, B. Representative examples of PARPi-FL labeling, PARP1 expression and corresponding H&E in two tissue sections, C. Quantification of average intensity and area positivity at image-level (log transformed data),  $p < 0.001$  for area positivity,  $p < 0.408$  for case-wise intensity, D, E. Quantification of average intensity and area positivity (no log transformation of data) at case-level (C) and image-level (D).

**Supplemental Figure 4.** A, B. Representative examples of RCM and FCM mosaics that highlight the utility of PARPi-FL in differential labeling of BCC tumors (yellow arrows) and hair follicles (green asterisk), enhancing tumor visualization on FCM, as compared to RCM, C. Representative example demonstrating absence of nuclear staining in nodular-cystic BCC tumor, D. Representative example of infiltrative BCC with heterogenous staining in BCC nests.

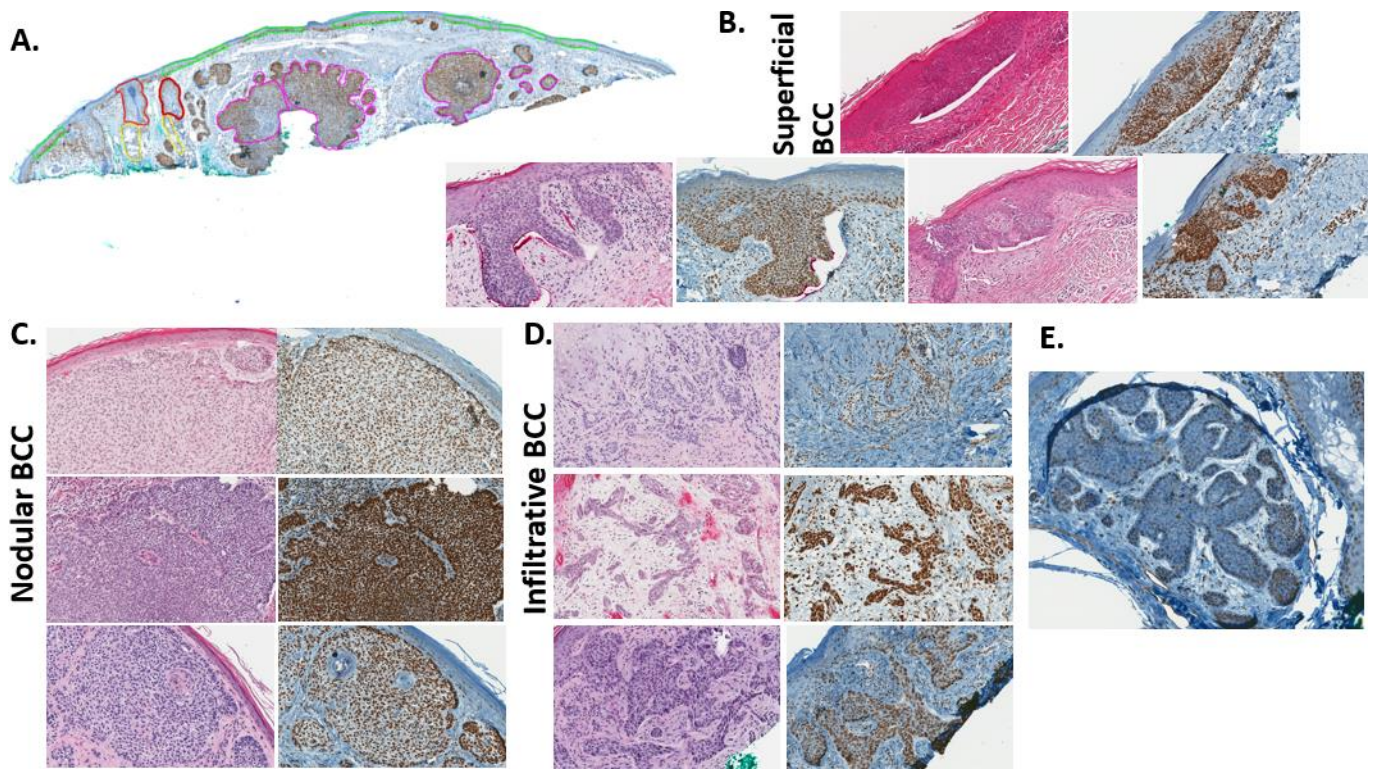
**Supplemental Figure 5.** A. Topical application of PARPi-FL (1  $\mu$ m for 10 minutes) through saturated gauze in human ex vivo tissue shows positive nuclear staining in epidermis and dermis following

permeation and passive diffusion (DAPI-blue) in pseudo colored images, B. Representative FCM from the in vivo pig experiment (inset). FCM image demonstrates positive nuclear staining in the basal layer of epidermis in test (PARPi-FL) image.

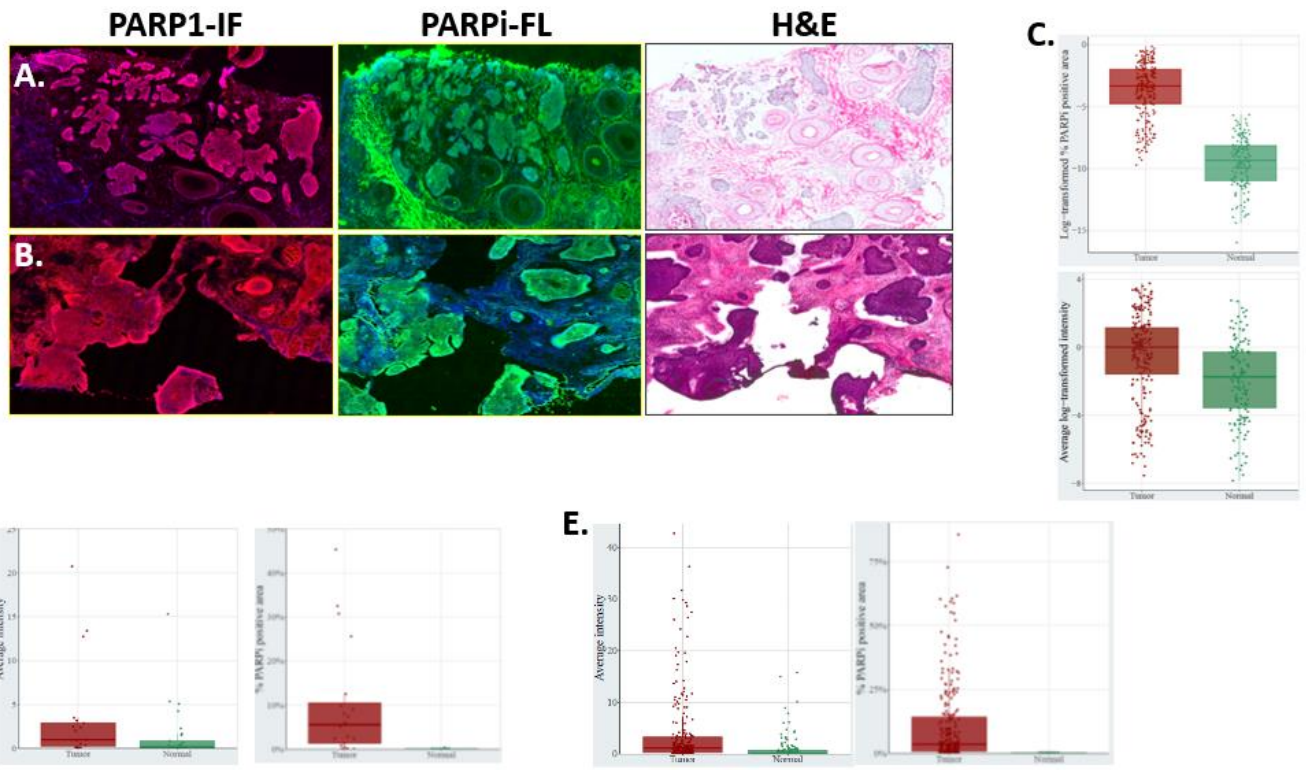
**Supplemental Figure 6.** A. Fresh normal and BCC tissue from surgical excision immersed in PARPi-FL (1  $\mu$ M for 30 minutes) or PEG-PBS solution, B, C. Experiments in normal tissue and BCC demonstrate no subsequent effect on histopathological processing and evaluation, and tissue structures, D. Statistical analysis for feature prevalence and agreement indicate matched prevalence of BCC tissues in both groups, and high interrater agreement for BCC diagnosis and staining quality.



Supplemental Figure 1.

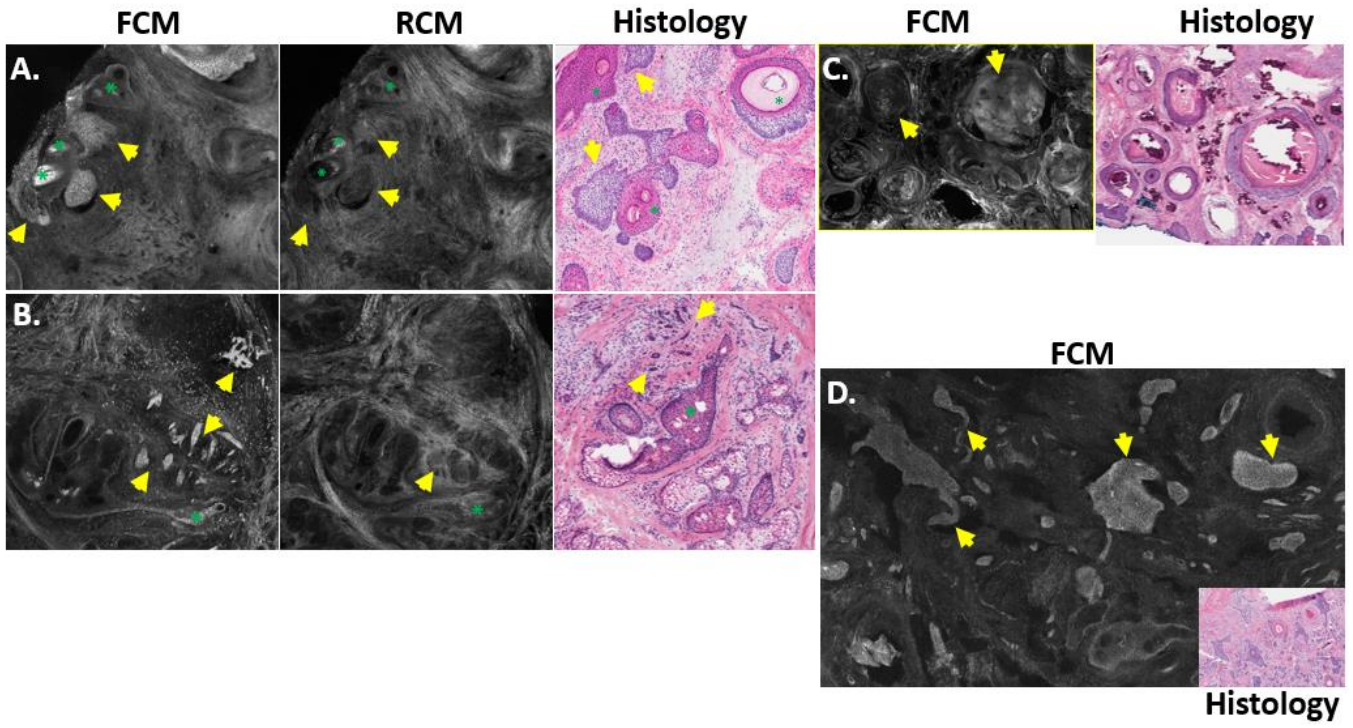


Supplemental Figure 2.

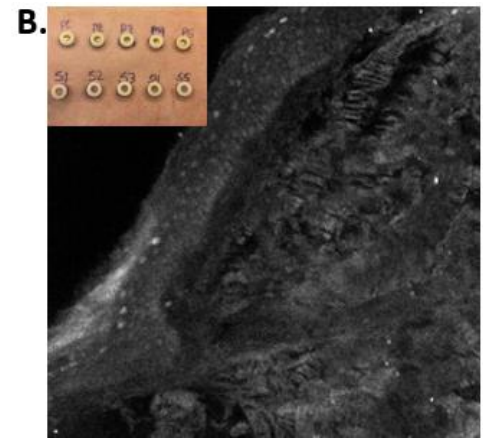
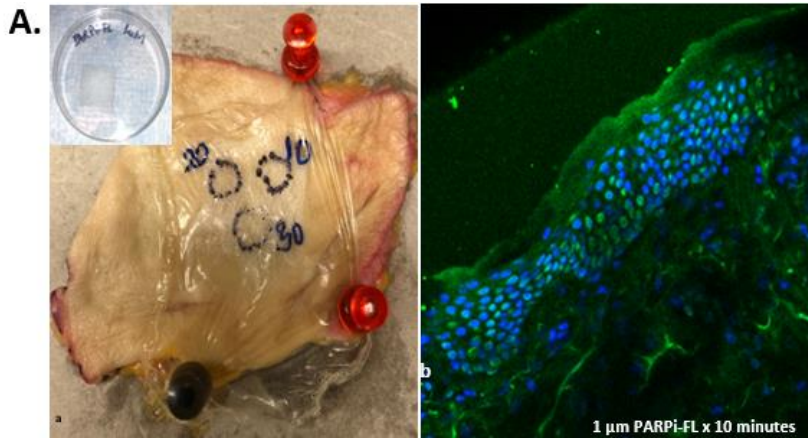


**Supplemental Figure 3.**

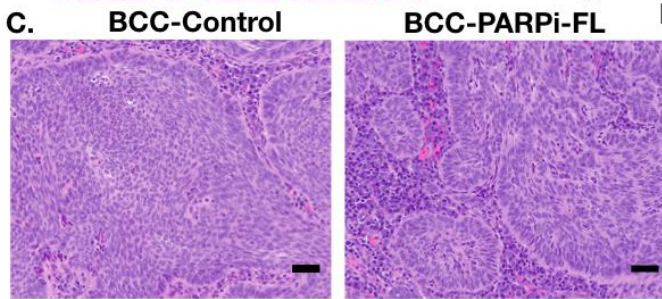
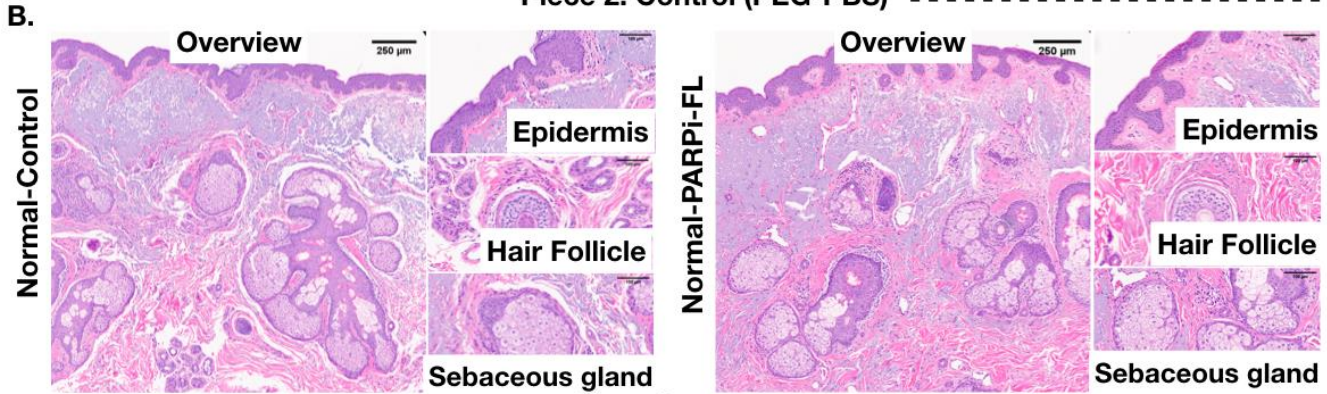
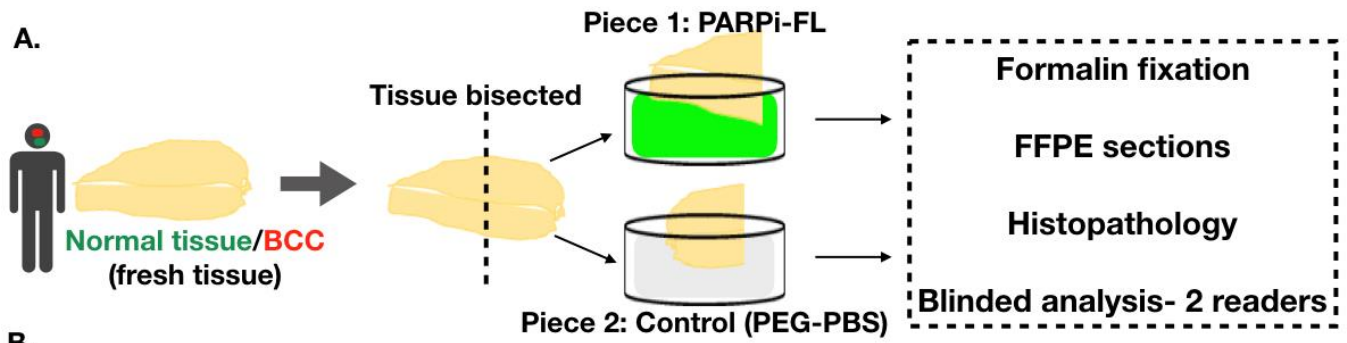




Supplemental Figure 4.



Supplemental Figure 5.



**D.**

Feature	Feature %		Interrater agreement			
	Solution		Parpi-FL		Saline	
	Parpi	Saline	%	Gwet's	%	Gwet's
Tumor	74	75	89	0.81	90	0.84
BCC						
-Superficial	30	40	80	0.66	60	0.23
-Nodular	45	55	90	0.8	70	0.4
-Invasive	35	35	90	0.92	90	0.82
Acceptable	100	100	100	1	100	1
Acceptable	100	100	100	1	100	1
Acceptable	100	100	100	1	100	1

Supplemental Figure 6.